

Singularities of Principal Direction Fields from 3-D Images

Peter T. Sander, *Member, IEEE*, and Steven W. Zucker, *Fellow, IEEE*

Abstract—Generic singularities can provide position-independent information about the qualitative shape of surfaces. We determine the singularities of the principal direction fields of a surface (its umbilic points) from a computation of the index of the fields. We present examples both for 3-D synthetic images to which noise has been added and for clinical magnetic resonance (MR) images.

Index Terms—Computational vision, differential geometry, direction field index, generic singularities, principal curvature and direction fields, 3-D image analysis, umbilic points.

I. INTRODUCTION

THE ACCURACY of structure estimated from images is necessarily guided by the demands of the eventual application. For description or identification of objects, qualitative but stable features can be more important than the precision required for quantitative analysis. In this paper, we present steps toward such a qualitative description by providing a computational method for the determination of umbilic points (second derivative singularities) of surfaces. In a companion article [2], we showed that the initial estimation of smooth differential structure from 3-D (e.g., magnetic resonance) images was sensitive to noise and, hence, required a subsequent refinement procedure to yield robust results. Here, we show that such a refinement is a required prerequisite for the reliable determination of singularities of the differential structure as well.

The critical points of a function are those points of its domain where the first derivative is zero. Although defined by the first derivative, critical points are characterized by second derivative properties; they are extrema (minima, maxima) or inflexion (saddle) points, depending on whether the Hessian matrix is positive definite, negative definite, or indefinite, respectively. Furthermore, critical points whose Hessian has a nonvanishing determinant are generic. Intuitively, this means that they are stable since a small perturbation of the surface in the region of the point yields a surface with qualitatively similar critical points. Points with zero determinant are unstable since small perturbations of the surface change the

Manuscript received May 4, 1988; revised January 8, 1991. This work was supported by NSERC Grant A4470 and MRC Grant MA 6125. Recommended for acceptance by W. E. L. Grimson.

P. T. Sander is with the Institute National de Recherche en Informatique et en Automatique, Unité de Recherche Sophia-Antipolis, Valbonne, France.

S. W. Zucker is with the McGill Research Centre for Intelligent Machines, McGill University, Montreal, Canada H3A 2A7.

IEEE Log Number 9102100.

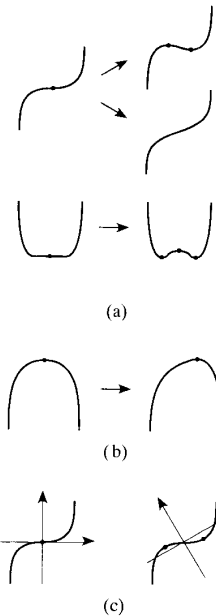


Fig. 1. (a) Critical points are unstable since a small perturbation of the function changes their number and type; (b) stable critical point whose character remains unchanged by a small perturbation of the function; (c) type of the critical point depends on the orientation of the curve in space; however, the critical point of the first derivative, that is, the zero of the curvature, is unchanged by rotation of the axes.

nature of the critical points. A simple example of stable and unstable critical points of functions is given in Fig. 1.

It is clear that critical points of functions depend on the coordinate system in which the functions are described (see Fig. 1(c)). Critical points of the derivatives of functions, however, do not depend on the embedding. Such second derivative properties can thus be more useful for orientation-independent descriptions. Two types of second derivative critical points of surfaces are parabolic points, which are those zeros of Gaussian curvature (critical points of the Gauss map) that appear on smooth surfaces between regions of elliptic and hyperbolic points [3], and umbilic points, which are the singularities of the direction fields. In this paper, we discuss only umbilic points. We show that the straightforward mathematical definition of umbilics as points with equal principal curvatures does not translate well into a computational procedure—point properties are by themselves insufficient—but that an algorithm can be developed from analysis of the direction fields over local neighborhoods, i.e.,

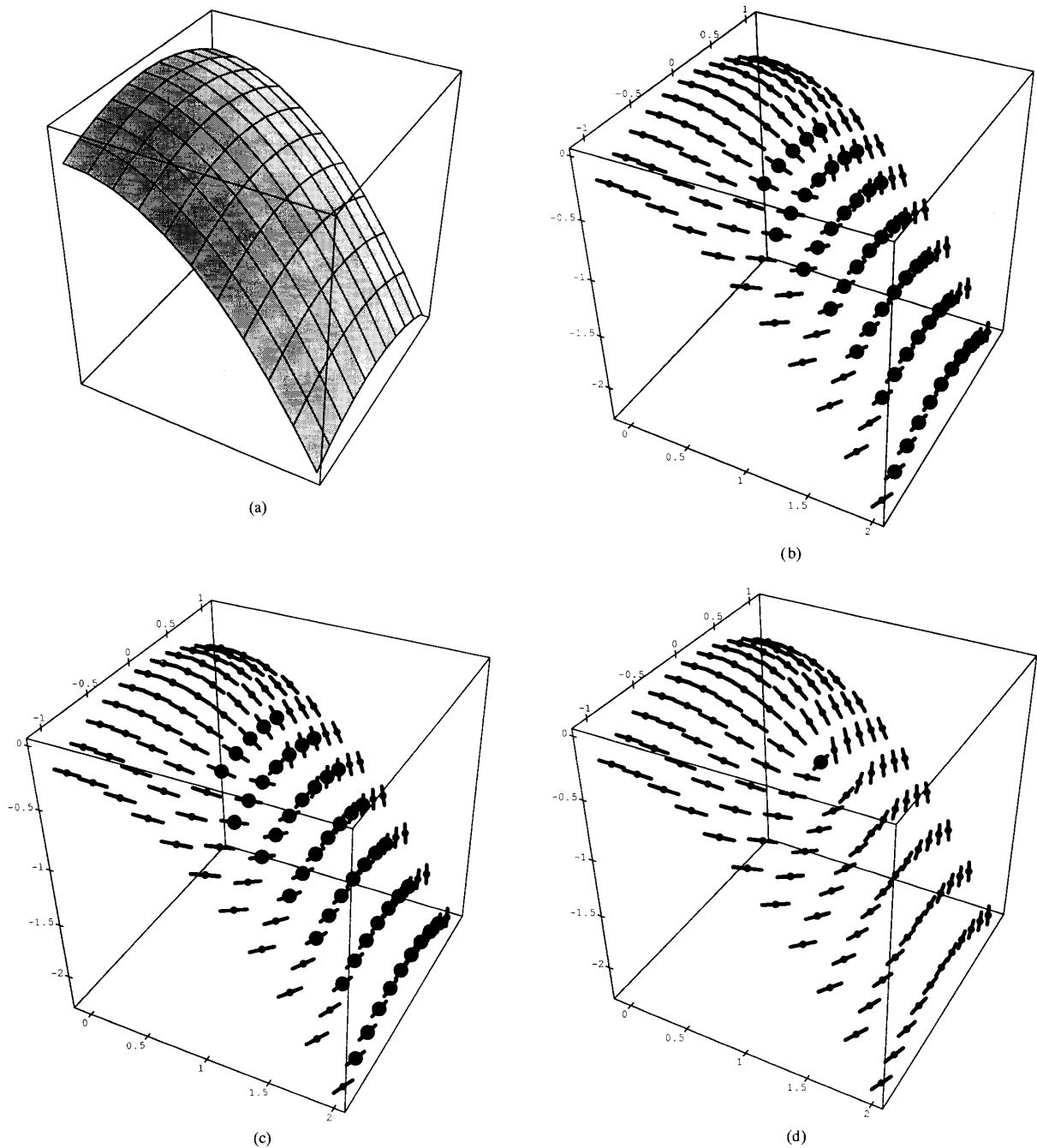


Fig. 2. Umbilic points determined on the surface of an elliptic paraboloid by thresholding the principal curvatures $|\kappa_M - \kappa_m| < \epsilon$: (a) Tangent plane orientations; (b) $\epsilon = 0.15$; (c) $\epsilon = 0.1$; (d) $\epsilon = 0.05$. Which threshold is correct, and how to set it?

from the computation of the index of the field. Umbilic points, considered as singularities of the principal direction fields, thus provide a link between local differential and global topological properties of surfaces (recall that by the Poincaré-Hopf index theorem [4], the sum of the indices of a smooth vector field with only isolated singularities on a compact oriented surface equals the Euler characteristic of the surface). It is

just such qualitative but stable properties that are emerging as fundamental to the robust description of surfaces [5].

Umbilic points of surfaces are of theoretical interest since the computation of lines of curvature by integrating the principal direction fields becomes complicated at those singularities. In addition, we believe that they are also of more direct interest as generic features that may be useful for matching surfaces

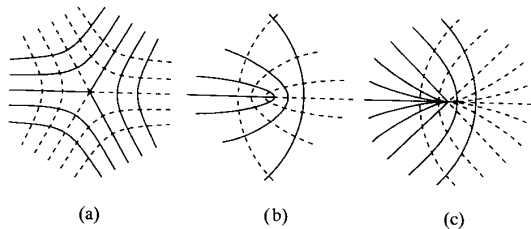


Fig. 3. Two classifications of umbilics [15]: (a) “Star” umbilic with index $-1/2$; (b) “lemon” with index $+1/2$; (c) “monstar” with index $+1/2$. The lines indicate the orthogonal net of lines of curvature with the solid and dashed lines belonging to the different families. See also [17].

of objects. For example, we are currently investigating their application to matching 3-D magnetic resonance (MR) images taken from different views and for matching individual patient data with an atlas of standard structures.

In the next section, we provide a summary of related work. Section III-B-3 discusses briefly the computation of local differential information and the refinement methods necessary to ensure robustness of the derived structures. Mathematical preliminaries concerning the characterization of umbilics are in Section III-A, although we assume familiarity with the notions of principal curvatures and directions. Section III-B presents the determination of umbilic points by computation of the index of the direction fields and gives examples of the application of our methods to both synthetic images degraded by noise and to clinical MR images.

II. RELATED WORK

Work related directly to that which we present here comes mostly from the analysis of rangefinder images, where the image can be considered as a bivariate function $I : U \subset \mathbb{R}^2 \rightarrow \mathbb{R}$, and object surfaces are already explicit in the form of the data. Surfaces in 3-D scanner images are one step removed since their trace points are only given implicitly and must first be extracted from the embedding 3-space.

Haralick *et al.* [6] are concerned with the determination of stable singularities of the first derivative of bivariate functions.¹ Such analysis says little about the intrinsic shape of objects as it depends on the situation of the objects in space (see also Nackman [7]).

Besl and Jain [8] provide an introduction to the differential geometry of surfaces and especially their second derivative properties; however, they express some doubts as to the feasibility of the stable computation of principal direction fields in real images and do not deal with singularities.

Koenderink and van Doorn [9] talk about Gaussian curvature zero crossings (parabolic lines) that separate elliptic and hyperbolic regions. Principal curvatures and directions have been recognized (by Faugeras and Hebert [10] among others) as important for shape analysis.

Brady *et al.* [11] determine second derivative properties and determine regions of umbilic points (in highly symmetric fabricated objects) but restrict their attention to certain isolated lines on surfaces, e.g., lines of curvature that are also planar. In

¹The roots of this approach can be traced at least back to Maxwell [16].

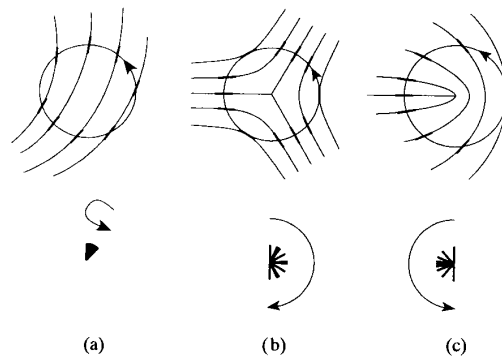


Fig. 4. Index of a point of a vector field is the total rotation experienced by a vector aligned with the field in a counterclockwise circuit about the point: (a) Index is zero where the direction field is smooth, but (b) is $-1/2$ at a star and (c) $+1/2$ at a lemon umbilic.

contrast, we take the approach of computing isolated, generic singular points from fields of principal directions. Stable singularities have also recently been studied in the analysis of general viewing positions and the behavior of the projections of the bounding curves onto the imaging plane [12].

Kass and Witkin [13] analyze oriented patterns in grey-level images and provide examples of the detection of singularities based on the direction field index. However, these fields exist on a plane surface given *a priori* and thus do not require the estimation of the location in space of the field points themselves.

III. UMBILICS

A. Characterization

In elementary differential geometry [14], umbilic points are generally introduced only as those points where the principal curvatures are equal. As is apparent in Fig. 2, however, localizing umbilic points in sampled images is more than just a matter of thresholding the principal curvatures κ_1, κ_2 by computing whether $|\kappa_1 - \kappa_2| \leq \epsilon$. Since it is likely that the “actual” umbilics will fall between the pixel grid points, the structure of the principal direction field should be taken into account. The analysis of the local field structure around umbilic singularities² presented in this section leads to a computational algorithm in Section III-B.

Although umbilics of surfaces are defined by second derivative properties, they are characterized by the third derivative as follows. The Taylor expansion terms of a local surface mapping $\mathbf{r} : U \subset \mathbb{R}^2 \rightarrow \mathbb{R}^3$ at P can be expressed simply in the appropriate (local tangent plane) coordinates [2], and we consider the terms truncated up to third order

$$\mathbf{r}(u, v) = \left(u, v, \frac{1}{2}(au^2 + cv^2) + \frac{1}{6}(au^3 + 3\beta u^2v + 3\gamma uv^2 + \delta v^3) \right). \quad (1)$$

At an umbilic point, i.e., where the principal curvatures are equal ($a = c$), the cubic coefficients $\alpha, \beta, \gamma, \delta$ determine its classification. Again, we are only interested in isolated umbilic

²Direction field vectors are always unit length so that, contrary to vector fields where the singularity is actually the zero vector, a unique direction field vector fails to exist at singular points.

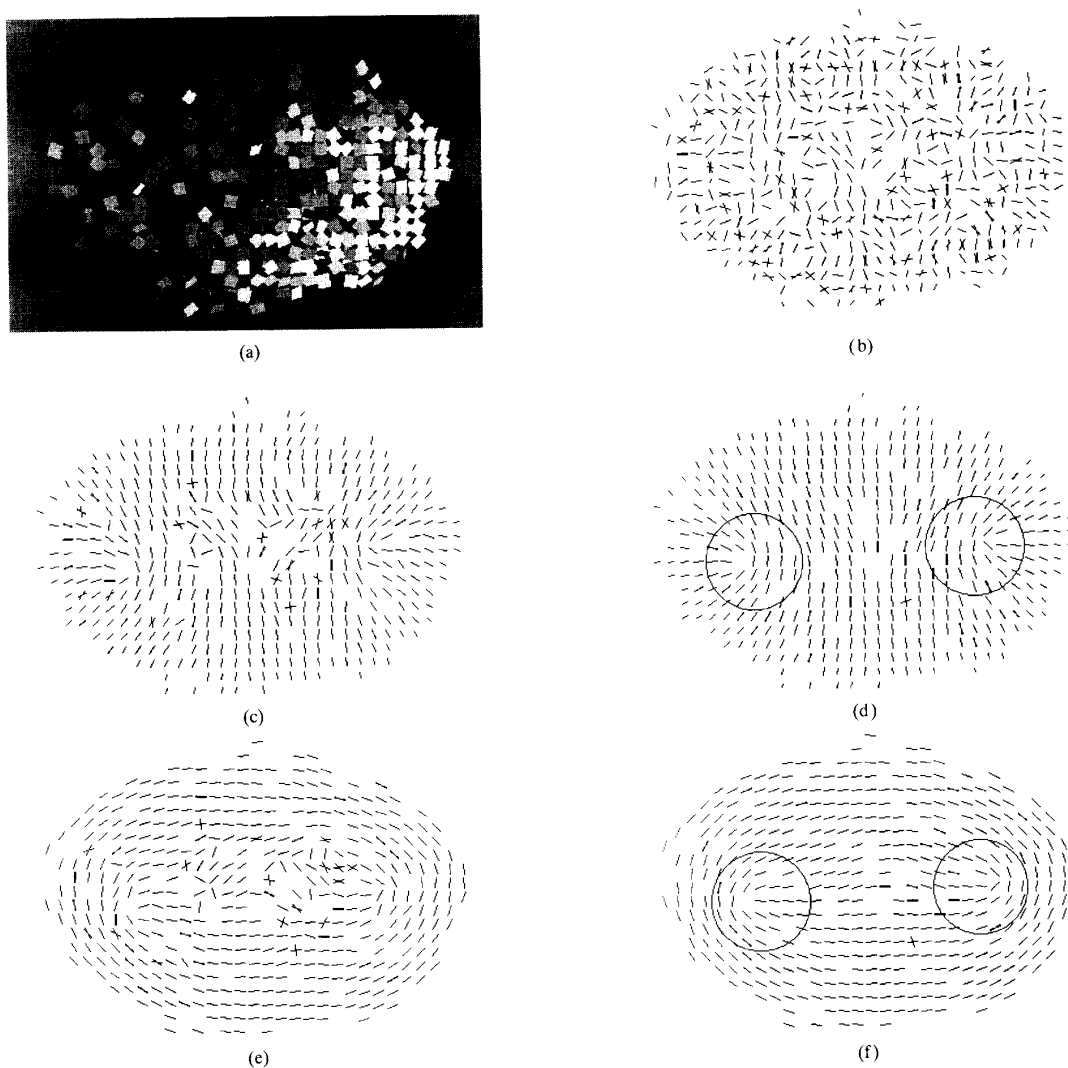


Fig. 5. Recovery of umbilics on the surface of an ellipsoid degraded by zero mean Gaussian noise with a variance of 0.33 added to both the tangent plane locations and orientations: (a) Orientation of the noisy tangent planes is indicated by the shading; the light source is from the lower right; (b) initial estimates of one of the principal direction fields; (c), (d) principal direction field after three and six refinement iterations. The superimposed circles show the circuit for the index computation around two umbilic points with index $+1/2$; (e), (f) three and six iterations over the other principal direction field. The hidden side has a similar structure, yielding an estimate of four lemon umbilics (see Fig. 195 of 3); (g) estimation of the index from the initial fields of (b); (h) umbilics recovered from (f); white indicates index $+1/2$, grey is index zero. No attempt has been made to further localize "the" umbilic, e.g., by shrinking the region of white points.

points that are generic, that is, stable to small perturbations of the surface.

Such generic umbilic surface singularities can be classified according to different criteria [15], of which two are of interest to us here (see Fig. 3):

- 1) By the configuration of the lines of curvature in the neighborhood of the umbilic: star, lemon, monstar
- 2) by the index of the umbilic: $\pm 1/2$. The index of a direction field at a point is $1/2\pi \int_0^{2\pi} \psi(\mathbf{r}) d\mathbf{r}$, where $\psi(\mathbf{r})$ is the angle between the direction of the field and some fixed direction, and the integral is taken over a small counterclockwise circuit about the point.

Star umbilics have index $-1/2$, and the other types have index $+1/2$.

B. Computation

The characterization of umbilics presents the same practical difficulties for implementation, as did their definition as points with equal principal curvatures. The classification follows from formulae using the cubic coefficients of (1) [15]. For example, the index could be computed directly from the discriminant

$$\text{if } \alpha\gamma - \gamma^2 + \beta\delta - \beta^2 \begin{cases} > 0, & \text{then index} = +\frac{1}{2} \\ < 0, & \text{then index} = -\frac{1}{2} \end{cases} \quad (2)$$

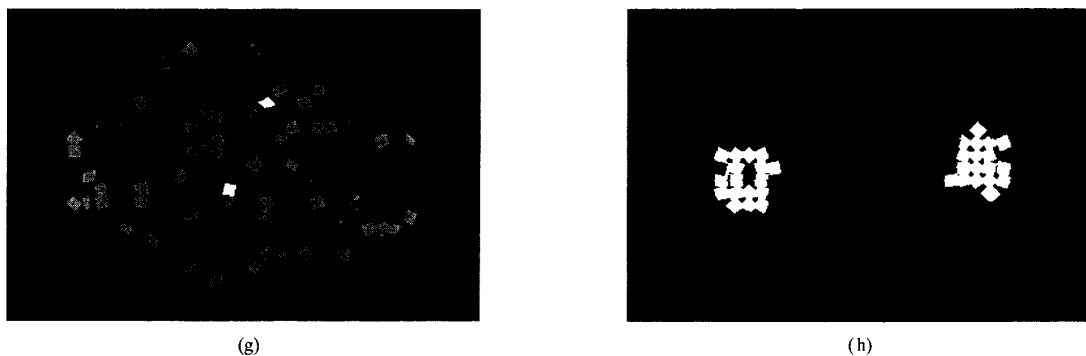


Fig. 5. (continued)

provided that we are certain that the discriminant is actually being computed at an umbilic. Since nonumbilics have vanishing index, the discriminant at nonumbilics is zero—but what is exactly zero in applications? The solution is to compute the index by taking into account the local structure of the direction fields. As we show below, in addition to classification, this permits identification of umbilics in a more robust fashion than does simply thresholding the principal curvatures.

1) *Principal Frame Fields*: Our aim is to infer from 3-D images the direction field singularities over estimated surface trace points, and in this section, we briefly sketch our method for obtaining the direction field estimates themselves (see [2] for a more complete treatment). A *frame* at surface point P is a 4-tuple $\xi_P = (P, \vec{e}_1, \vec{e}_2, \vec{e}_3) \in \mathbb{R}^{4 \times 3}$, where the three vectors $(\vec{e}_1, \vec{e}_2, \vec{e}_3)$ form a right-handed orthonormal system, and a *frame field* is a smooth mapping of a frame to each surface point. The principal direction fields are then composed of frames where \vec{e}_1, \vec{e}_2 are principal directions, \vec{e}_3 is the surface normal, and the normal curvatures κ_1, κ_2 of the surface at P are associated with the directions \vec{e}_1, \vec{e}_2 , respectively. We call this the *principal frame field*. In the application, we estimate an initial principal frame field from local (quadric) surface models fit at putative trace points (estimated by a 3-D gradient operator).

2) *Index Computation*: The principal frame field gives a net of two orthogonal principal direction fields on the surface. At “most” points, each field will be locally smooth, but at umbilics, the normal surface curvatures are equal in all directions, and hence, no distinguished principal directions exist. The *index* of the direction field at P is, informally, the total number of counterclockwise rotations that a direction vector undergoes in a small counterclockwise circuit about P (see Fig. 4). Thus, the implementation of the definition of the index provides an alternative to computation of the discriminant (see (2)). Let (r, θ) be the polar coordinates of a point on the circuit of fixed radius³ r centered at P and w.r.t. some fixed direction. Then

```

 $\theta := 0$ 
 $\Psi := 0$ 
do
   $\Psi := \Psi + \Delta\psi(r, \theta + \Delta\theta)$ 
   $\theta := \theta + \Delta\theta$ 

```

³All examples use circuit diameter $2r = 7$.

```

until  $\theta \geq 2\pi$ 
index: =  $\frac{\Psi}{2\pi}$ 

```

where

- $\Delta\theta$ is the incremental angle of the counterclockwise circuit.
- $\psi(r, \theta)$ is the angle of the direction field at circuit point (r, θ) with respect to the fixed direction; hence, $\Delta\psi(r, \theta + \Delta\theta)$ is the change in the field direction for the incremental step around the circuit from (r, θ) to $(r, \theta + \Delta\theta)$.
- Ψ is the cumulative change of the field direction w.r.t. the direction of the field at the initial point of the circuit.

The computations are simplified by pulling the field back onto the tangent plane of the point and computing the circuit there (which does not alter the qualitative character of the field [4]).

Computation of the index over a local neighborhood provides a conclusive test for umbilics—if the index is zero, no umbilic is present. However, as shown by the results, noise in the principal frame fields can also affect this (semi-) local computation; in the following section, we therefore suggest a refinement process for locally estimated principal direction fields.

3) *Refinement of Principal Frame Fields*: Given an imperfect estimate of principal frames of the surface \mathcal{S} , how is a better estimate made? The answer can be phrased within the calculus of variations: set up an appropriate global objective functional $\Phi : \Sigma \rightarrow \mathbb{R}$ over the space Σ of possible frame fields of \mathcal{S} , which will be minimized by the principal frame field. We implement such a minimization as an iterative constraint satisfaction algorithm, where the local information at P (its estimated principal curvatures and principal frame) is subject to smoothness constraints applied by the estimated structure at neighboring surface points Q_α as follows:

```

i := 0
do /* iteration step i*/
  i := i + 1
  forall P ∈ S
    determine appropriate neighborhood of P
    forall Qα ∈ neighborhood
      compute a new principal frame ξPαi at P
  end
  compute the new frame ξPi at P, which minimizes
  R(ξPi, {ξPαi})

```

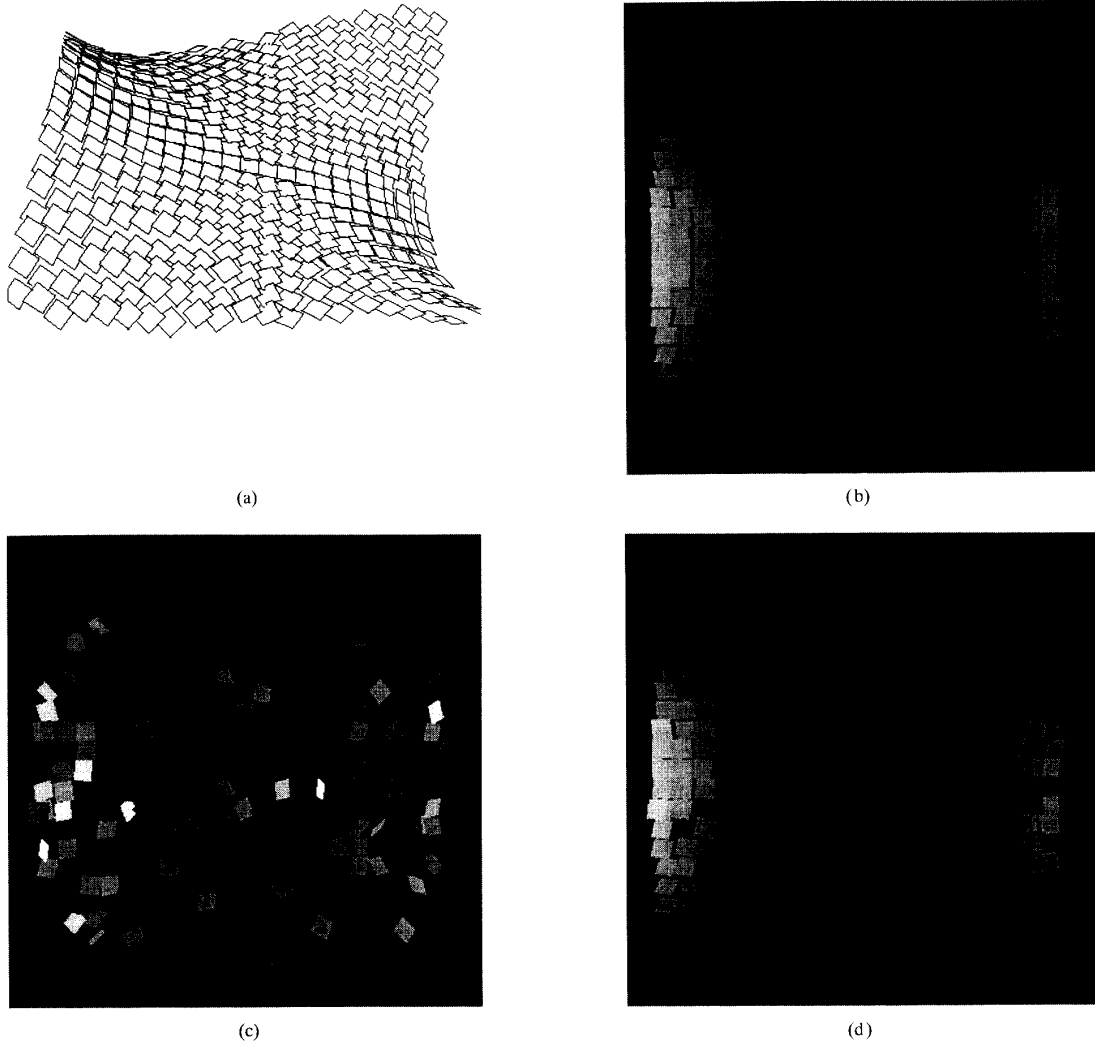


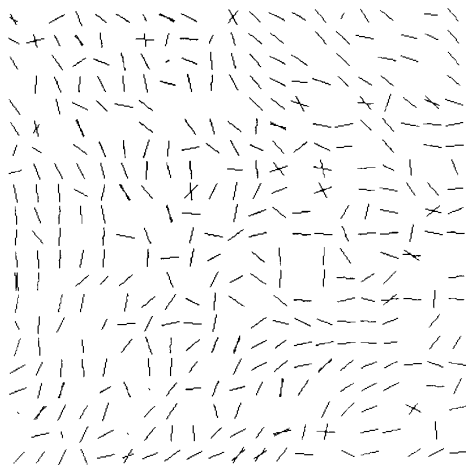
Fig. 6. Estimation of a star type umbilic on a noisy surface: (a) Tangent planes of the initial surface patch (a monkey saddle) tilted slightly in the viewing plane; (b) shading shows the orientation of the planes; the light source is from the right. With the same light source; (c) initial estimates on the noisy surface; (d) after six refinement iterations. One of the principal direction fields; (e) initially, (f) after six iterations; (g), (h) index computations on the initial field and on the refined field, respectively. Black points are index $-1/2$, grey points are zero, and white points are $+1/2$.

end
 until $\Phi(\{\xi_P^{i-1}\}_{P \in \mathcal{S}}) - \Phi(\{\xi_P^i\}_{P \in \mathcal{S}}) \approx 0$.

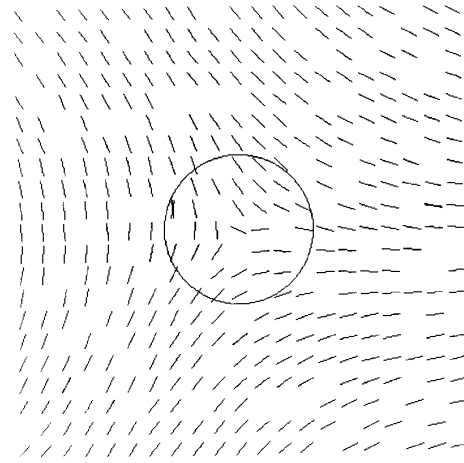
At iteration step i for each surface point P , the algorithm minimizes a local functional $R(\xi_P^i, \{\xi_{P\alpha}^i\}_\alpha)$ of the mismatch (i.e., maximizes the consistency) between the new principal frame ξ_P^i at P and the frames of the supporting neighborhood by computing ξ_P^i to be the "best fit" frame determined by its neighbors Q_α . Specifically, each neighborhood point Q_α determines a frame $\xi_{P\alpha}^i$ at P from its own local information, and the new frame ξ_P^i at P then becomes the least mean square error fit to $\{\xi_{P\alpha}^i\}_\alpha$. Note that consistency here involves relations between information at the same level among neighboring points; curvature information is determined from supporting curvature information rather than from tangent information as for the second derivative, for example. One

iteration step over all the points of \mathcal{S} then results in $\{\xi_P^i\}_{P \in \mathcal{S}}$, which is better in the sense of being a locally more consistent principal direction field over the surface.

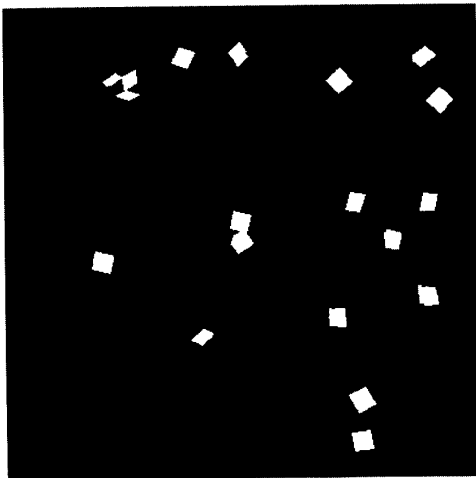
Thus, the global functional $\Phi(\{\xi_P^i\}_{P \in \mathcal{S}}) = \sum_P \sum_{Q_\alpha} R(\xi_P^i, \{\xi_{P\alpha}^i\}_\alpha) \geq 0$ depends on the consistency of the local information at each P with the local information over a neighborhood of supporting points. Increasing constraint satisfaction at each P thus leads to decreasing Φ , and when the total is small, the resultant field is a satisfactory estimate of the principal directions at each trace point. Finally, at iteration convergence, the computed local information can admit two complementary forms of grouping [2]: 1) integration of the estimated principal directions into lines of curvature and 2) grouping of points into patches with qualitatively similar Gaussian and mean curvature type.



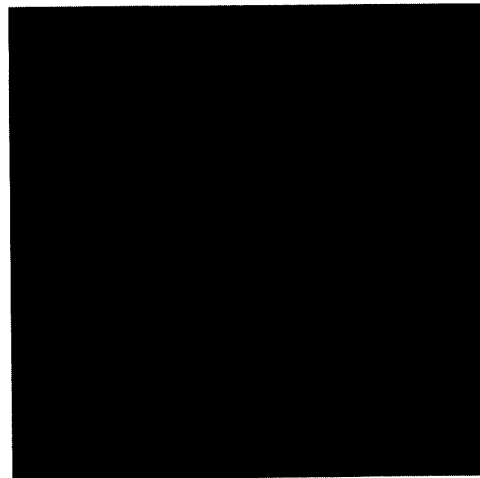
(e)



(f)



(g)



(h)

Fig. 6. (continued)

IV. RESULTS

Figs. 5–7 show that the local information refinement methods are necessary for the effective recovery of the differential structure in the neighborhood of isolated singularities. Further, they demonstrate the need for such refinement procedures for the computation of the direction field singularities (umbilic points) in noisy and real images.

Fig. 5 shows the correctness of the algorithm on a (sampled) smooth compact surface (an ellipsoid), whose tangent planes have been degraded by the addition of i.i.d. Gaussian noise (to both their position and orientation). Theoretically,⁴ the ellipsoid possesses four lemon umbilics (for a total index of 2, which is equal to its Euler characteristic), and all four are qualitatively recovered. We show all points with their indices computed by the algorithm of the previous section; we have

⁴By Poincaré-Hopf, the total number of umbilics over any surface with Euler characteristic $\chi = 2$ (topologically equivalent to a sphere) must have four star umbilics (each with index $-1/2$) less than the total number of umbilics of the other two types (with index $+1/2$).

made no attempt to localize “the” umbilic point within the region. Observe in (g) and (h) that it is only after refinement of the direction fields that the index computation is meaningful.

An umbilic of star type is estimated in Fig. 6 over a noisy surface patch. Notice again that local information refinement is necessary to even estimate locations of possible umbilic points. The example also shows that the algorithm does not smooth singularities off the edges of the surface patch.

The final example (Fig. 7) shows the index computation in the clinical MR image in the region of the bridge of the nose. Note the approximate symmetry between the umbilics found in the left and right halves separated by the nose. As with the synthetic images, the index computation is meaningful only once a certain coherence has been established in the direction fields by means of the refinement operations of the previous section.

V. CONCLUSIONS

Umbilic points are of interest for two reasons. First, as singularities of the principal direction fields, they will cause

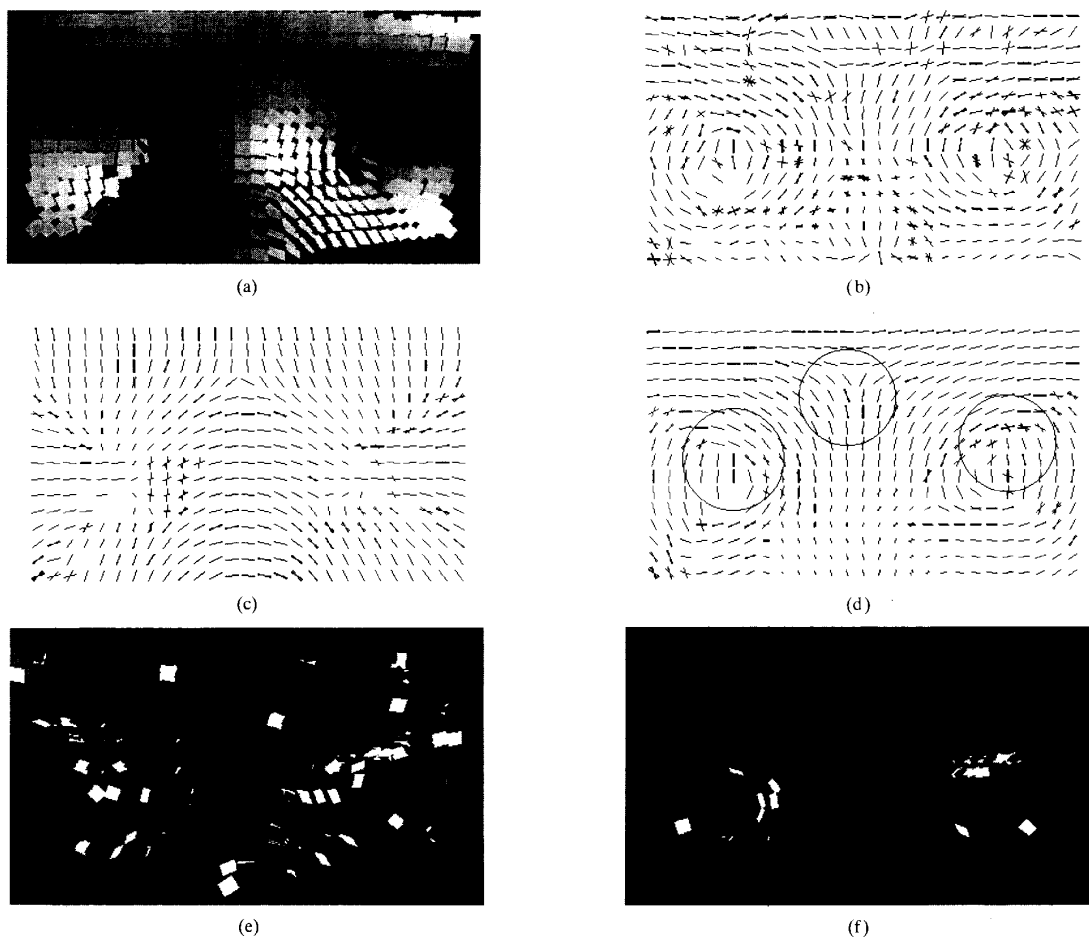


Fig. 7. Refinement of the principal direction fields around umbilic points in the face region of the magnetic resonance image: (a) Shading indicates orientation of the tangent planes—the light source is at the right; (b) initial estimates of one of the principal direction fields; (c), (d) both direction fields after six iterations (b) and (d) are the same field). The circles indicate circuits of the index computation algorithm around three singular points; (e), (f) index computations over the initial and the refined fields, respectively. Black points indicate star umbilics (with index $-1/2$), and white points are lemons (with index $+1/2$). Note that the index computations are approximately symmetric between the left and right halves.

difficulties for integrating the fields into lines of curvature. Knowing that umbilics are present alerts the integrator that special action may be needed, e.g., switching from directions associated with one principal curvature to directions associated with the other. Second, they provide distinguished surface features that are generic in the sense of being stable to small surface perturbations.

In this paper, we have argued that computation of umbilic points is unreliable from their original mathematical definition since this is based on thresholding the principal curvatures. Consideration of the umbilic points as singularities of the principal direction fields leads to the notion of index, which is computed over finite neighborhoods and serves to detect and characterize umbilics.

We have presented examples showing the detection and classification of umbilics that demonstrate the robustness of our method in the presence of noise.

We are currently further investigating umbilic points within a whole family of possible surface singularities, including

parabolic lines, focal surfaces, ridge lines, etc. We are also interested in determining how accurately our methods serve to estimate such singularities from realistic (noisy) data in the applications of these generic features to segmentation and matching problems.

REFERENCES

- [1] P. T. Sander, "On reliably inferring differential structure from three-dimensional images," Ph.D. thesis, McGill Univ., 1988; available as Tech. Rep. CIM-88-1, McGill Res. Cent. Intell. Mach., McGill Univ., Montreal, Canada.
- [2] P. T. Sander and S. W. Zucker, "Inferring surface trace and differential structure from 3-D images," *IEEE Trans. Patt. Anal. Machine Intell.*, vol. PAMI-12, no. 9, pp. 853–854, Sept. 1990.
- [3] D. Hilbert and S. Cohn-Vossen, *Geometry and the Imagination*. New York: Chelsea, 1952.
- [4] V. Guillemin and A. Pollack, *Differential Topology*. Englewood Cliffs, NJ: Prentice-Hall, 1974.
- [5] S. W. Zucker, "The emerging paradigm of computational vision," *Ann. Rev. Comput. Sci.*, pp. 69–89, 1987.
- [6] R. M. Haralick, L. T. Watson, and T. J. Laffey, "The topographic primal sketch," *Int. J. Robotics Res.*, vol. 2, pp. 50–70, Spring 1983.

- [7] L. R. Nackman, "Two-dimensional critical points configuration graphs," *IEEE Trans. Patt. Anal. Machine Intell.*, vol. PAMI-6, no. 4, pp. 442-450, 1984.
- [8] P. Besl and R. Jain, "Intrinsic and extrinsic surface characteristics," in *Proc. IEEE Comput. Vision Patt. Recogn.*, June 1985, pp. 226-233.
- [9] J. J. Koenderink and A. J. van Doorn, "The shape of smooth objects and the way contours end," *Perception*, vol. 11, pp. 129-137, 1982.
- [10] O. D. Faugeras and M. Hebert, "The representation, recognition, and locating of 3-D objects," *Int. J. Robotics Res.*, vol. 5, no. 3, pp. 27-52, Fall 1986.
- [11] M. Brady, J. Ponce, A. Yuille, and H. Asada, "Describing surfaces," in *Proc. Second Int. Symp. Robotics Res.*, 1986, pp. 5-16.
- [12] J. J. Koenderink, "The internal representation of solid shape and visual exploration," *Sensory Experience, Adaptation, and Perception* (Spillman and Wooten, Eds.). New York: Lawrence Erlbaum, 1984.
- [13] M. Kass and A. Witkin, "Analyzing oriented patterns," *Comput. Vision Graphics Image Processing*, vol. 37, pp. 362-385, 1987.
- [14] M. P. do Carmo, *Differential Geometry of Curves and Surfaces*. Englewood Cliffs, NJ: Prentice-Hall, 1976.
- [15] M. V. Berry and J. H. Hannay, "Umbilic points on Gaussian random surfaces," *J. Phys. A: Math. Gen.*, vol. 10, no. 11, pp. 1809-1821, 1977.
- [16] J. C. Maxwell, "On hills and dales," *London Edinburgh Dublin Philo. Mag. J. Sci.*, pp. 421-425, Dec. 1870; reprinted in *Scientific Papers of James Clerk Maxwell* (W. D. Niven Ed.). New York: Dover, 1965, pp. 233-240, 1965.
- [17] G. Darboux, *Leçons sur la Théorie Générale des Surfaces*. Paris: Gauthiers-Villars, 1896.



Peter T. Sander (S'80-M'88) received the B.Sc. degree in mathematics from Carleton University, Ottawa, Canada, the M.Sc. degree in computer science from the University of Western Ontario, London, Canada, and the Ph.D. degree in electrical engineering from McGill University, Montreal, Canada.

He is currently a professor at the École Supérieure en Sciences Informatiques of the Université de Nice-Sophia Antipolis, France, where he directs the Automatisme Industrielle et Robotique option and

the Robotics and Artificial Vision doctoral DEA program. He is also associated with the Informatique, Signaux, Systèmes à Sophia Antipolis Laboratory of the CNRS and with the Institut National de Recherche en Informatique et en Automatique. He is involved in biomedical image analysis and mobile robotics. His current research involves applications of differential geometry, differential topology, and singularity theory to problems in 3-D vision, with interest in aspects of multidimensional visualization.



Steven W. Zucker (F'88) received the Bachelor's degree from Carnegie-Mellon University, Pittsburgh, the Ph.D. degree at Drexel University, Philadelphia, and was a post-doctoral Research Fellow in computer science at the University of Maryland, College Park.

He was Professor Invité at Institut National de Recherche en Informatique et en Automatique, Sophia-Antipolis, France, in 1989. He is currently a Professor of Electrical Engineering at McGill University, Montreal, Canada, Director of the Program in Artificial Intelligence and Robotics of the Canadian Institute for Advanced Research, and Co-Director of the Computer Vision and Robotics Laboratory at the McGill Research Center for Intelligent Machines.

Dr. Zucker has authored or co-authored more than 130 papers on computational vision, image processing, artificial intelligence, biological perception, and robotics, and serves on the editorial boards of eight journals. He is a fellow of the Canadian Institute for Advanced Research.